Experiments in Fluids 18 (1995) 137–144 © Springer-Verlag 1995

Application of liquid-crystal thermometry to drop temperature measurements

T. Nozaki, T. Mochizuki, N. Kaji, Y. H. Mori

Abstract A technique has been developed that enables remote sensing of the temperatures of liquid drops in a medium of an immiscible, transparent liquid with the aid of dispersing microcapsules of thermochromic liquid crystal in each drop under illumination by either a planar floodlight or a light sheet which cuts the drop at a meridian. Based on appropriate hue–temperature calibrations made with an isothermal, stationary drop/medium system, one can analyze spatial and time variations of temperature within drops in motion under transient convective heating (or cooling) from the medium.

List of symbols

B	tristimulus blue component
D	drop diameter
G	tristimulus green component
H	hue angle
H_0	constant term in the expression for H
H_m	mean value of H over drop surface
h	vertical coordinate fixed onto test column
R	tristimulus red component
Re	drop Reynolds number, UD/ν_c
r, g, b	chromaticity coordinates
r	drop radius
s	penetration depth of light into drop
T	temperature
T_d	instantaneous drop temperature
T_{d0}	initial drop temperature
T_c	continuous-phase temperature
U	velocity of rise of drop
z	vertical coordinate laid on drop
ν_c	kinematic viscosity of continuous phase
θ	angle of lighting measured from camera axis
θ_s	local view angle (azimuth)
ϕ	polar angle

Received: 4 January 1994/Accepted: 24 May 1994

T. Nozaki
Dept. of Mechanical Engineering, Keio University,
3-14-1 Hiyoshi, Kohoku-ku,
Yokohama 223, Japan

T. Mochizuki
Mechanical Engineering Research Laboratory, Hitachi, Ltd.,
502 Kandatsu-cho,
Tsuchiura 300, Japan

N. Kaji
Dept. of Mechanical Engineering, The Polytechnic University,
4-1-1 Hashimoto-dai,
Sagamihara 229, Japan

Y. H. Mori
Dept. of Mechanical Engineering, Keio University,
3-14-1 Hiyoshi, Kohoku-ku,
Yokohama 223, Japan

Correspondence to: T. Nozaki

1 Introduction

Formation and translation of liquid drops in a continuous medium of another immiscible liquid are essential processes in a wide range of liquid–liquid contact operations including direct-contact heat transfer and liquid–liquid extraction. It is sometimes desired to determine the instantaneous temperatures of drops in those processes. For example, the knowledge of the change in the temperature of each drop, if available, will provide us with an adequate base for calculating the instantaneous rate of heat transfer to or from the drop and thereby evaluating the heat transfer coefficient.

The most conventional means for detecting the temperature of a drop in motion may be to place a fine thermocouple on the expected passage of the drop so that the drop will pass over the thermocouple junction. The most sophisticated version of this technique may be the one developed by Moresco and Marschall (1979), in which a computer-aided processing of the thermo-voltage-history data obtained with 50–100 drops sampled at a fixed location determines the mean and the surface temperatures of the drops at the location.

Despite such a refinement of the data acquisition/processing technique as outlined above, thermocouple thermometry is still under serious restrictions in practical use: it never provides the temperature histories of individual drops in motion, and it will no longer work well when drops follow nonrectilinear trajectories.

In view of the possibility of eliminating these restrictions, the infrared-rays radiant thermography, a widely-used remote sensing method, can be a good alternative to the thermocouple thermometry provided that the materials surrounding the drops are transparent to infrared radiation or the effect of absorption in those materials of the infrared rays from the drops is substantially eliminated. Unfortunately, no reliable means to eliminate or compensate the absorption in the liquid medium

holding the drops is available. Thus, IR thermography as it exists now is not suitable for liquid–liquid systems.

This paper describes an experimental examination addressed to another noncontact temperature measurement technique – liquid-crystal suspension thermometry which currently finds widening application in thermo-fluid science. The technique utilizes microcapsules of cholesteric or chiral nematic liquid crystals which change color reflection, when illuminated by a "white" light, in response to a temperature change. The microcapsules suspended in a liquid can serve not only as temperature sensors but also as tracers for flow visualization. It should be noted in this respect that the shear-stress dependencies of the color reflection behavior of the liquid crystals are apparently eliminated as the result of their encapsulation with some resins. The technique has been developed and tested since the 1980s by, for example, Rhee et al. (1984), Wilcox et al. (1985) and Dabiri and Gharib (1991). Measuring colors exhibited by the liquid crystals for determining temperatures quantitatively is a subject still awaiting better solutions. Dabiri and Gharib (1991) give a pertinent review of color-image processing techniques developed for this purpose up to 1990.

Having inspected the literature, we find no attempt having been made to measure drop temperature with liquid crystals. Drops have strong surface curvatures. In addition, they are generally in motion. These facts possibly add difficulties in composing optical systems for color-image acquisition and also in the color-image processing. In the present work, with focus placed on such yet overlooked matters which are essential to drop temperature measurements, practical techniques suitable for the measurements are being sought.

2
Experimental setup and procedure

Figure 1 illustrates the whole experimental setup we constructed to test the applicability of liquid-crystal suspension thermometry to measuring temperatures of single drops, which may be stationary (just as illustrated there) or translating. The setup is composed of a test column assembly, a drop-image acquisition system and a drop-image processing system. The test column is a rectangular vessel, 90-mm square in cross section, equipped with a nozzle for releasing drops at its bottom. The column is fabricated, together with a water jacket enclosing it, of transparent PMMA [poly(methyl methacrylate)] plates and is lined with opaque, black-colored PMMA plates, leaving a narrow band on each of its front and rear walls to permit only the light from a particular light source – a 300-W halogen lamp (3,200 K color temperature) of a slide projector behind the column – to illuminate drops in the column at a well-defined azimuth angle from the camera axis, θ (Fig. 2). Throughout the present experiments, a methylphenyl silicone oil (KF54 fluid prepared by Shin-etsu Chemical Co., Ltd., Tokyo) was used as the continuous-phase liquid to fill the column, while a volume of water suspending microcapsules of a chiral nematic liquid crystal was used to form drops in the silicone oil. The temperature of the silicone oil was held constant and uniform at a desired level by circulating temperature-controlled water through the jacket enclosing the column. The temperature of the water suspending the liquid crystal capsules could be adjusted to some different level before its issuing from the nozzle by circulating another

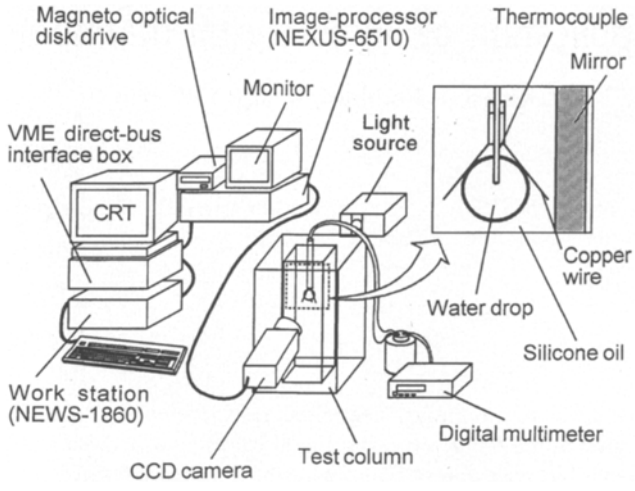

Fig. 1. Schematic of experimental setup. Each drop may be held stationary as illustrated here or released to buoy up freely

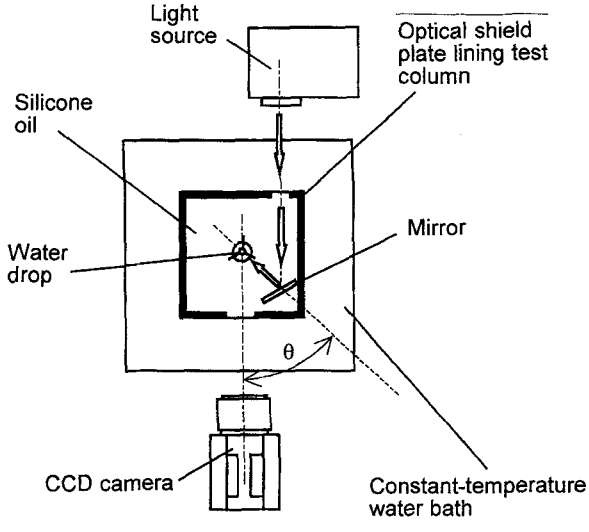

Fig. 2. Optical geometry for drop image recording (plan view)

source of temperature-controlled water through the jacket enclosing the nozzle.

The drop-image acquisition system consists of the slide projector serving as a white-light source and a three-chip CCD color video camera set across the column from the projector. The projector is used either alone to provide a diverging floodlight for illuminating the entire front surface of each water drop or together with a slit–lens assembly to form a plane, vertically spread light sheet about 1 mm thick, which is meant to illuminate a meridian of the drop. In either case, the light is once reflected before its incidence upon the drop by a plane mirror vertically immersed in the silicone oil. The camera-view angle relative to the axis of illumination, θ, is varied by turning the mirror on a vertical axis. The 3-chip CCD camera (Sony DXC-3000A) is adjusted to 3,200 K color temperature, while the gain of the CCD sensor is set to be invariable with any possible change in the intensity of illumination. For viewing each drop at an appropriate magnification, a 35-mm camera lens (Canon

New FD 85mm, 1.2 L) is attached to the CCD camera using a specially-made adapter.

The drop-image processing system mainly consists of an image processor (Nexus-6510) and a host computer (Sony News-1860 work station) connected with each other via a VME direct-bus interface. A magneto-optical disk drive (Sony NWP-559) is attached to the processor for storing many yet-to-be processed images of stationary drops. The MO disk drive is replaced by a video tape recorder when dealing with moving drops. Each drop image captured by the camera as separate *R*, *G* and *B* images is once stored in the magneto-optical disk or the video tape recorder and then inputted into the processor, in which each of the *R*, *G* and *B* images is digitized to 256 gradations (8 bit) with 512×480 pixels.

Various procedures of color image processing exist which may be applicable to color-to-temperature conversion. Having reviewed the procedures examined in previous works, Dabiri and Gharib (1991) recommended the [*H* (hue), *S* (saturation), *I* (intensity)] representation of the (*R*, *G*, *B*) color space, which may be achieved by transforming the *RGB* signals from a CCD camera to (*X*, *Y*, *Z*) primaries based on the 1931 CIE (Commission International de l'Eclairage) color system, then to (*Y*, *u*, *v*) indices defined in the 1960 CIE uniform chromaticity scale system, and finally to (U^*, V^*, W^*) indices characterizing the 1964 CIE uniform color space to which *H* and *S* are related directly. The procedure we have selected follows Dabiri and Gharib's recommendation in quantifying *H*. However, we have bypassed the complicated coordinate transformations in the course of calculating *H* by assuming the *RGB* values read on the processor to be the tristimulus values conforming the CIE *XYZ* color system. This assumption permits us to evaluate the chromaticities – *r*, *g* and *b* – simply as:

$$r = R/(R+G+B)$$
$$g = G/(R+G+B) \quad (1)$$
$$b = B/(R+G+B)$$

These *r*, *g* and *b* values are then used to calculate *H* as

$$H = \tan^{-1}\left[\frac{\sqrt{3}(g-b)}{2r-g-b}\right] + H_0 \quad (2)$$

where H_0 is zero whenever the first term on the right side has a positive value but it expresses 2π (360°) when the first term has a negative value.

It should be noted that what is critical to liquid-crystal thermometry is not the absolute "accuracy" but the "precision" both in calibrating *H* against known *T* and in observing some target (a drop or some portion of a drop) of yet-to-be determined temperature. The precision may be estimated from the results of *H*–*T* calibrations presented in the following section.

3
Color–temperature calibrations with drops at uniform temperatures

Calibrations of drop color images against temperature have been made with isolated water drops each held stationary in the isothermal silicone oil medium by a three-fingered drop catcher made of three copper wires (Fig. 1). Microcapsules ~15 μm in diameter encapsulating a chiral nematic liquid crystal with a ureaformaldehyde resin film (KWN-42 or KRN-42 prepared by Japan Capsular Products Inc., Tokyo) were added at 0.05 wt% to distilled water from which the drops were formed. Under illumination from behind an observer ($\theta = 0°$), the KWN-42 capsules were said to give reflections in red, green and blue at 37.0, 40.9 and 45.6 °C, respectively, and the KRN-42 capsules were to do so at 42.0, 42.7 and 43.7 °C (manufacturer's data). The purpose of the present calibrations was to reveal how such chromatic reflections vary with θ, the angle of illumination (Fig. 2), the location within the illuminated area on each drop, and drop size over the entire color-reflecting temperature range. The reference temperature in each calibration with a particular drop was obtained with a copper–constantan thermocouple 0.5 mm in diameter inserted into the drop through the drop-catcher support (Fig. 1). Each image of the drop captured by the camera was stored in the image processor in the form of an image file.

Figure 3 exemplifies an image of a water drop illuminated by a light sheet at $\theta = 90°$. Here we find that the color exhibited by the liquid crystal capsules appreciably changes along the path of the light sheet crossing the drop from right to left. In contrast, little change in color is noted along a vertical axis. For quantifying the above-mentioned spatial variation in color, five small areas, each covering 50×50 pixels, symmetrically distributed on the drop image (see the inset in Fig. 4) were processed separately to evaluate local hue angles at the positions of those sample areas. Hue angle vs. temperature plots thus obtained are shown in Fig. 4. It should be noted here that the response in hue to a temperature rise tends to be suppressed with an increase in the penetration depth of the light into the drop as if, in view of the θ dependency of the hue–temperature relation demonstrated below, the local azimuth angle of the light measured from the camera axis decreased with increasing penetration depth. The tendency is ascribable to refractions, at the frontal drop surface, of the rays which are reflected on liquid crystal capsules and finally (due to the very refractions) directed to the camera. As illustrated in Fig. 5, the local view angle measured from the incident light axis, θ_s, is larger than θ when the penetration depth of the light, *s*, is less than the drop radius *r*, but it decreases below θ as *s* exceeds *r*.

Figure 6 shows variations in the hue–temperature relation with θ. The illumination is in the form of either a light sheet intersecting the drop center [graph (a)] or a flood light [graph (b)]. The hue angles indicated by discrete dots in either graph are those evaluated over 50×50 pixels at the center of the drop image – i.e., the drop center in (a) but some point on, or just beneath, the equator of the drop in (b). A spline interpolation procedure incorporating a least-squares curve-fitting algorithm has been applied to the experimental data (the dots in the graphs) to prepare reference hue–temperature correlations which are represented by solid curves. Irrespective of the form of illumination, the hue vs. temperature plots show essentially the same dependency on θ. The temperature range in which the liquid crystal capsules exhibit temperature-dependent color reflections (varying from red, $H = 0$, at the lowest temperature to blue, $H \approx 240°$, at the highest temperature) tends to broaden and, at the same time, to shift toward higher temperatures with a decrease in θ. This fact means that the temperature range measurable with given liquid crystal capsules is variable to some

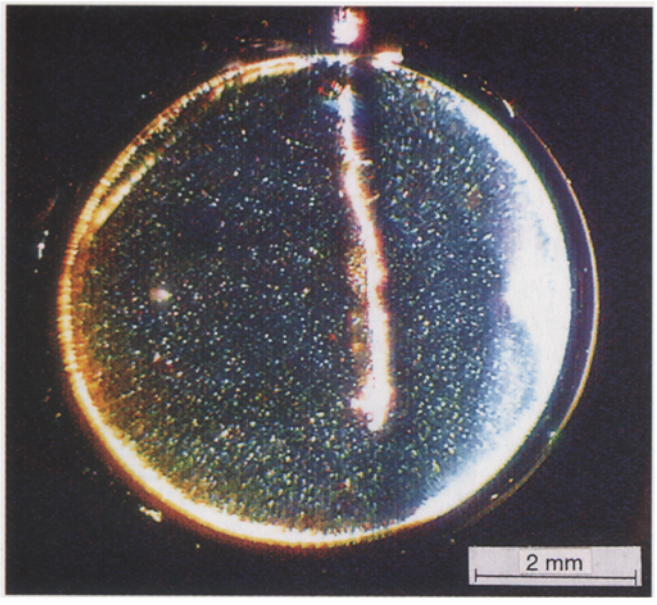

Fig. 3

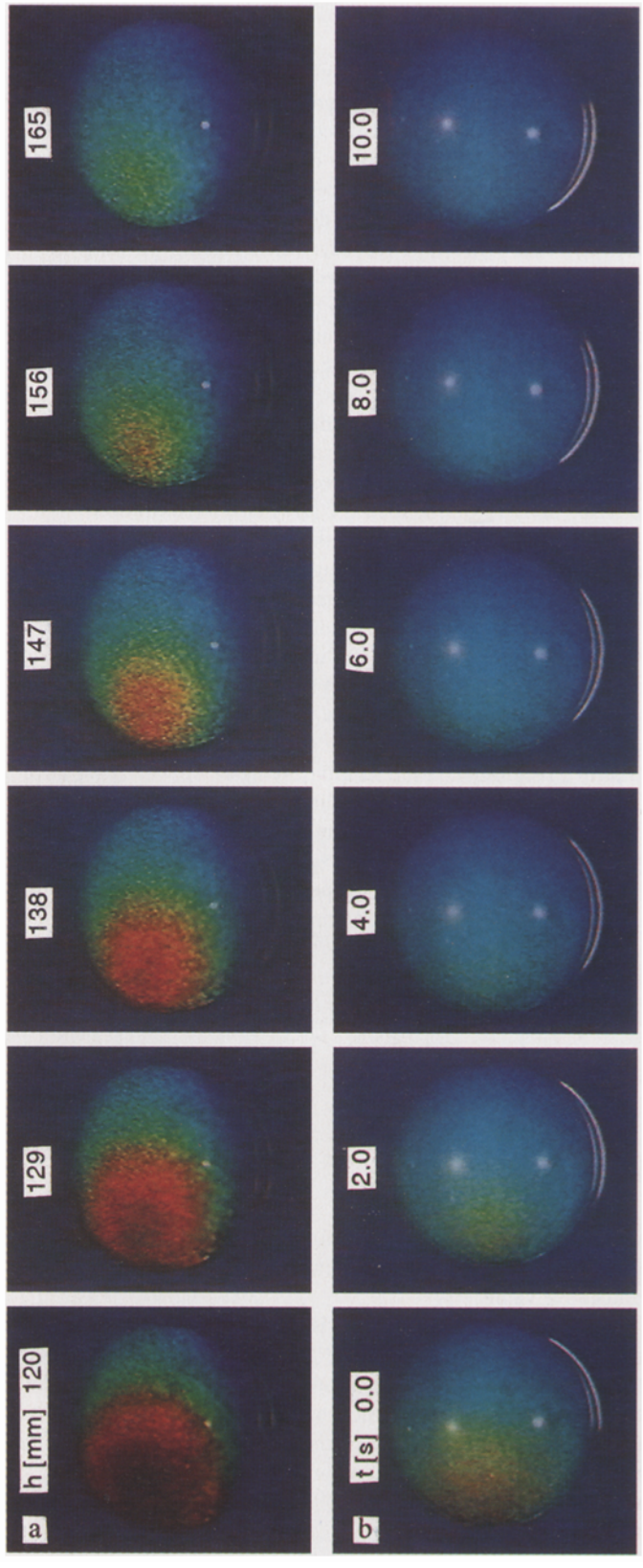

Fig. 8

Fig. 3. Drop image under illumination with a light sheet directed from right to left. $\theta = 90°$. The drop contains KWN-42 capsules. The temperature is uniform (35.7 °C)

Fig. 8a, b. Change in color image of a drop during free rise. Either a light sheet (**a**) or a floodlight (**b**) was provided from right to left at $\theta = 45°$. h is a vertical coordinate directed upward. Note that h- and t-values are common to the horizontally opposed panels in (**a**) and (**b**)

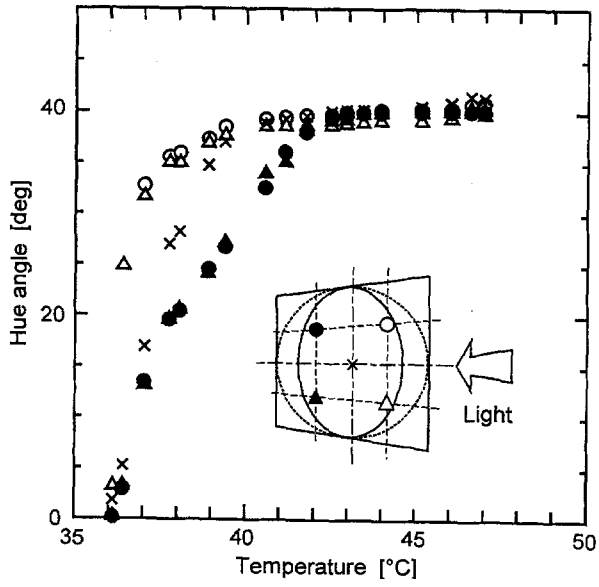

Fig. 4. Hue vs. temperature relations obtained with a drop (6.2 mm in diameter) which contained KWN-42 capsules and was illuminated with a light sheet at $\theta = 60°$

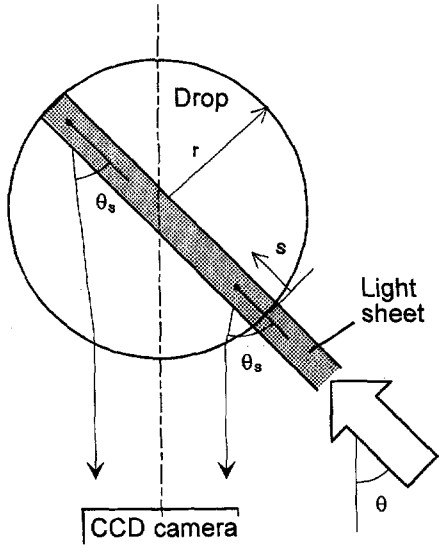

Fig. 5. Schematic illustrating variation of local view angle (azimuth) θ_s with penetration depth of light sheet into drop, s. Note that $\theta_s > \theta$ when $s < r$, and vice versa

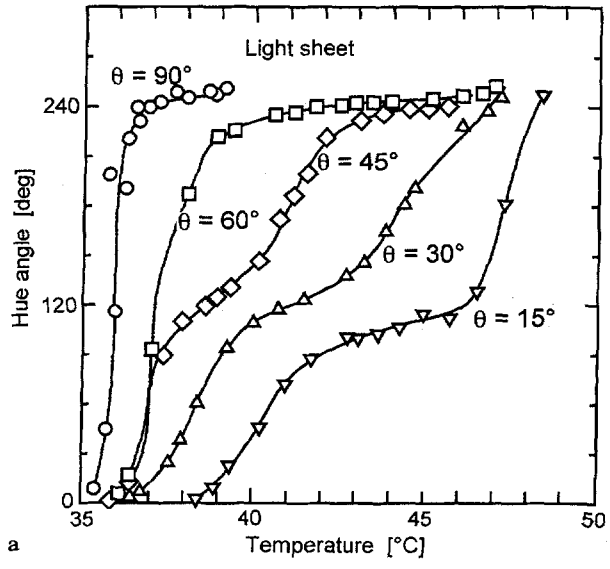

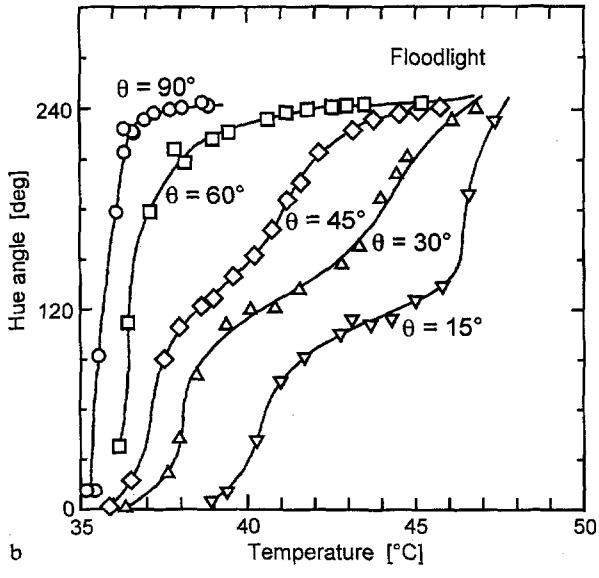

Fig. 6a, b. Variation of hue (at center of drop image) vs. temperature relation with the angle of illumination, θ. The data were obtained with drops 6.5 mm in diameter that contained KWN-42 capsules

extent provided that we can alter the angle of illumination, θ. Although the hue–temperature relation is significantly nonlinear no matter how we vary θ, it still ensures that the hue is a single-valued function of temperature and the temperature is also a single-valued function of the hue at any angle in the range $15° \leqslant \theta \leqslant 90°$. Thus, it may be said that the range $15° \leqslant \theta \leqslant 90°$ is, in principle, usable for temperature measurements with liquid crystal capsules.

In practice, however, reasonable accuracy of measurements is guaranteed only when dH/dT is not too small where T denotes the temperature to be measured. Sufficient sensitivity to temperature variations of the order of ± 0.1 K is available when dH/dT is larger than some 20 deg/K. On the other hand, the width of the color-variable temperature range is generally important at the same time. In view of these circumstances, the illumination angle $\theta = 45°$ is recommended. This is considered to be a good compromise between the accuracy of measurement and the width of the measurable temperature range.

It is quite important to define the drop size over which the hue–temperature relation is practically drop-size-independent. There is a great technical difficulty in making a white-light sheet much thinner than 1 mm but still intense enough for giving clear color images. Thus, the use of a light sheet for obtaining images of a cutting plane intersecting the drop axis is necessarily limited to drops a few millimeters in diameter at the smallest. Figure 7 shows hue–temperature relations observed with drops from 2.9–8.2 mm in diameter under a light sheet set at $\theta = 45°$. Here we find little change in the hue–temperature relations

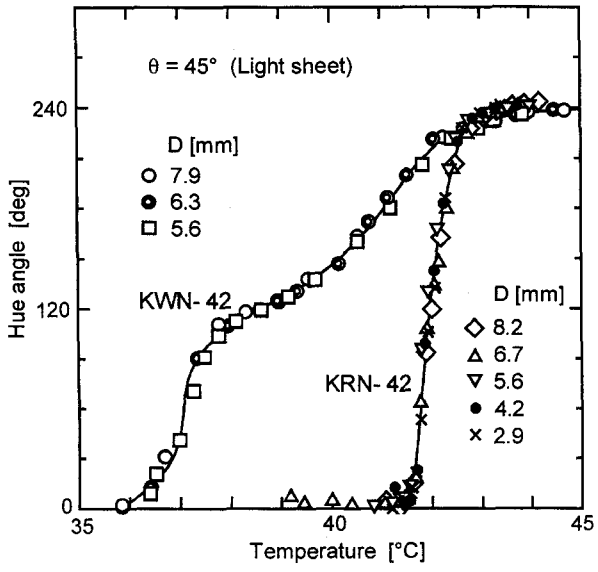

Fig. 7. Hue angle versus temperature. The data were obtained with drops 2.9–8.2 mm in diameter

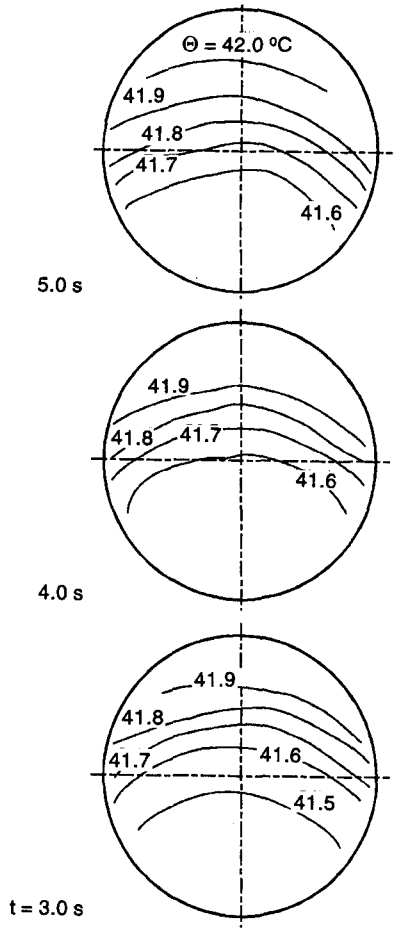

Fig. 9. Temperature distributions on a cutting plane intersecting the vertical drop axis. Prepared from color images shown in Fig. 8a

with the drop size. The applicability of a floodlight for getting near-surface images of drops possibly extends to a submillimeter diameter range.

The precision of the hue–temperature calibration data obtained with the illumination at $\theta = 45°$ is estimated to be within ± 5 deg in H for either KWN-42 and KRN-42 capsules. The least squares curve-fitting to the data is reasonably accurate in view of the precision of the data. The accuracies in reading temperatures based on the calibration curves for KWN-42 and for KRN-42 capsules are estimated to be ± 0.2 K ($0° \leqslant H \lesssim 230°$) and ± 0.1 K ($10° \lesssim H \lesssim 230°$), respectively.

4
Application to drops in free rise under transient heating

A series of experiments were carried out in which water drops containing KRN-42 capsules were released into the continuous phase of the silicone oil to undergo transient heating. A syringe-infusion pump was used to force the water out of the nozzle, thus forming drops of a uniform size ($D = 5.2 \pm 0.1$ mm) at a regular, sufficiently long interval. The temperature of the drop-forming water detected by a thermocouple inserted into the nozzle to a location just below the outlet, T_{d0}, was controlled at 36.6 ± 0.3 °C, while the undisturbed continuous-phase temperature, T_c, was maintained at 43.1 ± 0.2 °C. Each drop released from the nozzle rose in the quiescent medium of the silicone oil, undergoing a temperature rise due to the heat transfer from the medium. The path of the drop was rectilinear, and the speed of the rise became constant ($U \approx 4.4$ mm/s, $Re \approx 0.15$) after the rise of the first 120 mm above the nozzle outlet. A light sheet or a floodlight was used to illuminate drops at an azimuth angle, $\theta = 45°$.

Figure 8 shows two sequences captured with a light sheet and a floodlight, respectively, each of which represents a color-image history of a particular drop during its rise through some 50-mm span above the elevation $h = 120$ mm, where h is the vertical distance measured from the nozzle outlet. The color images aligned there clearly visualize the temperature distribution on a cutting plane or on the drop surface at each instant. Based on detailed hue–temperature calibrations at many positions over the plane or the surface under isothermal conditions, one can convert each of the color images such as those given in Fig. 8 into a map indicating a spatial temperature distribution on the plane or the surface. Some examples are presented in Fig. 9. It should be noted that each isotherm map in Fig. 9 results from not only the hue-to-temperature conversion on a corresponding color image of a cutting plane (Fig. 8a) but also a geometrical reconstruction of the image illustrated in Fig. 10: it consists of a "reorientation of the observer" to the azimuth normal to the cutting plane and corrections, in the radial coordinate, of the refractions of light rays at the drop surface such as those illustrated in Fig. 5. The geometrical reconstruction has been made in practice on the assumptions that the drop is spherical and that the visual angle of the drop observed through the camera is sufficiently small.

The isotherm maps illustrated in Fig. 9 indicate that the heat transfer inside the drops was mostly conductive. Although we did not notice some circulatory trajectories of liquid-crystal microcapsules inside each drop, the flow inside the drop was presumably too weak to yield an appreciable effect on the heat transfer. One may realize the dominancy of conduction in the internal heat transfer more clearly by comparing the isotherm maps in Fig. 9 with numerical solutions of the problem of

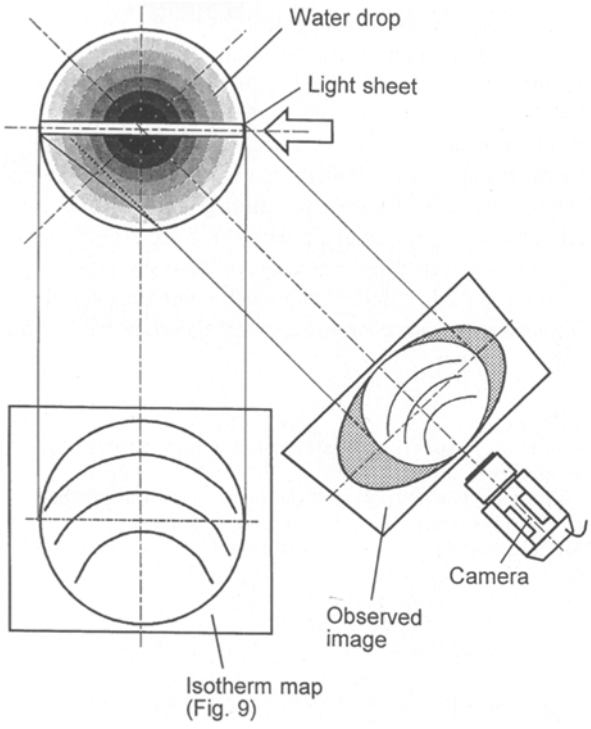

Fig. 10. Schematic illustrating geometrical reconstruction of observed images of a plane (or a planar layer) "cut out" by a light sheet

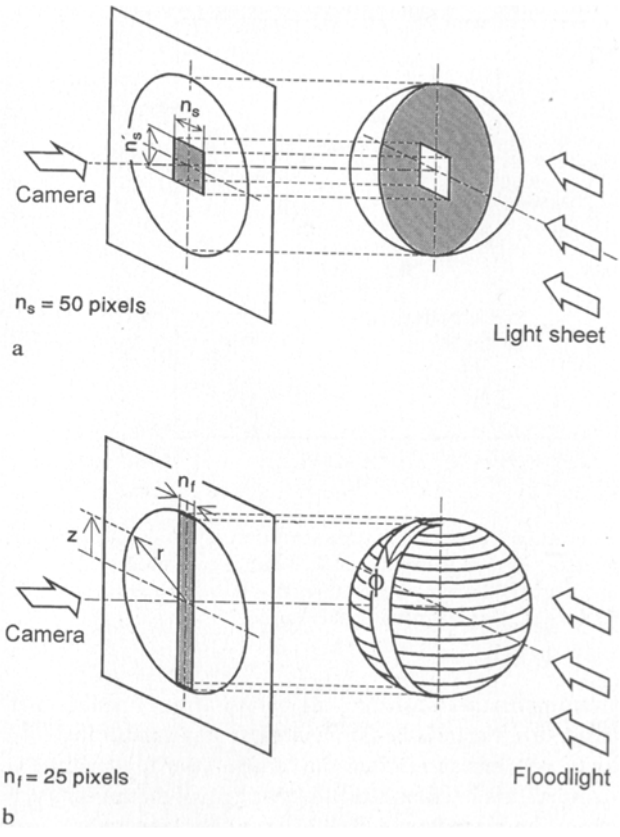

Fig. 11a, b. Illustrations of spatial regions assigned for image processing

conjugate heat transfer to or from a translating drop with or without internal circulation (see, for example, Abramzon and Borde, 1980).

If a complete map of the temperature distribution at an instant on a cutting plane intersecting the vertical drop axis is obtained, one can calculate the mixed-mean temperature of the drop at that instant on the assumption of an axisymmetric temperature distribution being established inside the drop at each instant. To obtain such complete maps, a technical contrivance may be required to determine temperature profiles right up to the drop surface with reasonable accuracy.

In some applications, we are required to know only the history of some (arbitrarily defined) reference temperature of a drop instead of the spatial temperature distribution at each instant. A typical case is when one intends to evaluate the overall coefficient of medium-to-drop (or drop-to-medium) heat transfer based on the time variation of drop temperature observed (see, for example, Kaji et al., 1978). In view of such circumstances, we show below how the transient behavior of a reference drop temperature, T_d, is deduced from the sequential color images demonstrated in Fig. 8.

For the images obtained with a light sheet, we define as the reference instantaneous drop temperature, T_d, the temperature corresponding to the hue angle averaged over the 50×50 pixels at the center of each drop image [Fig. 11a]. This temperature should approximate the temperature at the center of the drop. For the images obtained with a floodlight, we define as T_d the temperatures corresponding to H_m, the hue angle averaged over the entire drop surface. Here we need to introduce two assumptions: (1) the temperature distribution in the drop is axisymmetric and hence the surface temperature is a function of only the polar angle ϕ, and (2) the local hue angles $H(z)$ based on 25 pixels laterally aligned about the vertical center line of a drop image represent the hue angles $H(\phi)$ on the meridian on the drop surface facing the camera axis [see Fig. 11b]. With these assumptions, we can calculate H_m as

$$H_m = \frac{1}{4\pi r^2} \int_0^{\pi} 2\pi (r \sin\phi) H r \, d\phi = \frac{1}{2r} \int_{-r}^{r} H \, dz = \frac{1}{2} \int_{-1}^{1} H \, dZ \qquad (3)$$

where r is the drop radius, z is a vertical coordinate given by $r\cos\phi$, and $Z \equiv z/r$. H_m thus evaluated is converted into temperature according to the H–temperature correlation for the central area of drop image, which is based on a calibration performed with an isothermal system optically analogous to the present one.

The instantaneous drop temperatures thus evaluated are plotted in Fig. 12 in the form of a fractional approach of T_d to T_c, the continuous-phase temperature, with the vertical distance traveled by the drop. As expected, T_d evaluated on the basis of H_m shows a faster approach to T_c than the one converted from H at the core of the drop. The linear alignment of the data point in the semi-log diagram means that the instantaneous overall heat transfer coefficient is held constant during the rise of the drop (Kaji et al., 1978).

5 Concluding remarks

The present study has demonstrated the applicability of micro-encapsulated liquid-crystal thermometry to the quantitative measurements of instantaneous drop temperature during transient heat transfer processes. An empirical finding of

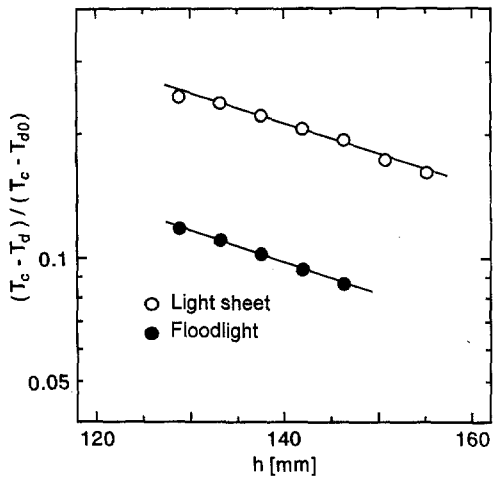

Fig. 12. Fractional approach of drop temperature to the continuous-phase temperature in the course of free rise of each drop. T_c = undisturbed medium temperature, T_d = instantaneous drop temperature, T_{d0} = initial drop temperature

practical importance regarding the optical arrangement is that the target drops should be illuminated at some acute angle (typically 45°), measured from the camera axis, at which the hue–temperature relation is the least wriggly. If the trajectory of each drop is accurately predictable, even the temperature distribution within the drop at each instant can be determined by capturing sequential color images obtained with a light sheet intersecting the drop axis. Some technical problems encountered in processing each color image into two-dimensional temperature distribution and the practical procedures to eliminate the problems have been described in this paper. The technical tasks still left to future study include constructing the computational algorithm for accurately calculating mixed-mean drop temperature from discrete local-temperature data deduced from each color image and developing a scheme for processing color images of nonspherical drops.

References

Abramzon B; Borde I (1980) Conjugate unsteady heat transfer from a droplet in creeping flow. AIChE J 26: 536–544

Dabiri D; Gharib M (1991) Digital particle image thermometry: the method and implementation. Exp Fluids 11: 77–86

Kaji N; Mori YH; Tochitani Y; Komotori K (1978) Direct-contact heat transfer to drops in an intermittent electric field. Proc 6th Int Heat Transfer Conf., Vol 3: 165–170

Moresco LL; Marschall E (1979) Temperature measurements in a liquid–liquid direct-contact heat exchanger. AIChE Symp Ser 75: 266–272

Rhee HS; Koseff JR; Street RL (1984) Flow visualization of a recirculating flow by rheoscopic liquid and liquid crystal techniques. Exp Fluids 2: 57–64

Wilcox NA; Watson AT; Tatterson GB (1985) Color/temperature calibrations for temperature sensitive tracer particles. Proc Int Symp on Physical Flow Visualization, Albuquerque, N.M., 65–74